Separation Science and Technology
Publication details, including instructions for authors and subscription information:
http://www.informaworld.com/smpp/title~content=t713708471

Performance of Gas Separator with High-Flux Polyimide Hollow Fiber Membrane

K. Haraya[a]; K. Obata[a]; T. Hakuta[a]; H. Yoshitome[a]
[a] NATIONAL CHEMICAL LABORATORY FOR INDUSTRY, IBARAKI, JAPAN

To cite this Article Haraya, K. , Obata, K. , Hakuta, T. and Yoshitome, H.(1988) 'Performance of Gas Separator with High-Flux Polyimide Hollow Fiber Membrane', Separation Science and Technology, 23: 4, 305 — 319
To link to this Article: DOI: 10.1080/01496398808060706
URL: http://dx.doi.org/10.1080/01496398808060706

SEPARATION SCIENCE AND TECHNOLOGY, **23**(4 & 5), pp. 305-319, 1988

Performance of Gas Separator with High-Flux Polyimide Hollow Fiber Membrane

K. HARAYA, K. OBATA, T. HAKUTA, and H. YOSHITOME

NATIONAL CHEMICAL LABORATORY FOR INDUSTRY
YATABE, TSUKUBA, IBARAKI, 305 JAPAN

Abstract

The permeation properties of H_2–CO mixtures through a high-flux asymmetric polyimide membrane are studied experimentally and theoretically. Experimental results measured with miniature module-equipped hollow fibers indicate the advantage of countercurrent flow pattern. The calculation model used for the analysis of the conventional symmetric membrane can predict the gas separation performance. However, the model is necessary to take the longitudinal mixing into account for analyzing the experimental results measured with a pilot scale module.

INTRODUCTION

By the development of high-flux asymmetric membranes composed of a surface skin layer and a porous substrate, applications of glassy polymer membranes, which have high selectivities but small permeabilities in general, have been successful for some gas separation processes. On the other hand, many modeling studies (*1–16*) clarifying the effect of idealized flow patterns of the feed and permeate streams and membrane configurations are available for designing an efficient separator.

Two recent investigations are notable for their design and analysis of a separator with an asymmetric glassy polymer membrane. One is the Chern et al. report (*17*) which introduces the dual-mode transport model as a permeation equation, whereas the constant permeability model was conventional. The other is Pan's report (*18*) in which he showed that there

is a substantial difference in separation performance between symmetric and asymmetric membranes, because local fluxes of the asymmetric membrane should be similar to the characteristics of the cross flow pattern regardless of the flow direction of the bulk permeate stream, i.e., the backdiffusion through the porous sublayer from the bulk permeate stream should be prevented by the high permeate flux.

These new concepts lead to results different from those of conventional studies. Specifically, it is worthwhile to consider Pan's model which greatly reduces the advantage of the countercurrent flow pattern. Moreover, it is forecast that the shell-side stream through a commercial-scale hollow fiber separator is not the ideal plug flow because of the longitudinal mixing. This effect also must be analyzed by a mathematical model [e.g., the partial mixing model by Hwang and Kammermeyer (*9*)]. In this paper, separation tests of H_2-CO mixtures with a miniature separator having a high-flux asymmetric polyimide hollow fiber membrane are examined experimentally and theoretically to determine whether the flow pattern effects exist. In addition, the experimental results of a pilot-scale separator are analyzed by a serial multistage model which takes longitudinal mixing into account.

ANALYSIS OF A MINIATURE SEPARATOR

Assumption

Model equations for cocurrent and countercurrent flow patterns were derived, based on the following assumptions.

(1) The gas mixture is fed into the shell side, and plug flow situations exist in both the high-pressure and low-pressure (permeate) streams.
(2) The deformation of the fiber under pressure is negligible.
(3) The porous sublayer has negligible resistance to permeation.
(4) The pressure drop in the fiber bore can be estimated by the Hagen-Poiseuille equation [Berman's study (*19*)], but is not taken into account along the embedded inactive section of the fiber.
(5) Permeation equations can be written using the constant permeabilities determined by permeations of the mixture.
(6) Concentration polarization near the membrane surface in the high-pressure stream is negligible. As a result of theoretical considerations (*20*), this assumption is valid in this experiment.

Using the above common assumptions, the following two models were examined.

Model A: The gas composition on the interface between the dense skin layer and the porous sublayer is equal to that of the bulk low-pressure stream because of rapid mixing by backdiffusion along the pore path. This model is identical with the one used for the prediction of the performance of conventional symmetric membranes.

Model B: The gas composition on the interface is controlled only by the fraction of local permeates of individual components because the backdiffusion is insignificant due to the high permeate flux [Pan's proposal (*18*)].

Material Balances and Working Equations

Figure 1 illustrates an idealized single hollow fiber membrane with an anisotropic structure. In the cocurrent flow mode the high-pressure stream outside the fiber flows as shown by the solid line arrows and the axial coordinate direction is taken as parallel to the flow. In the countercurrent flow mode, that flow and coordinate are reversed, as shown by the dashed line arrows.

Equations of material balances are summarized in Table 1 using

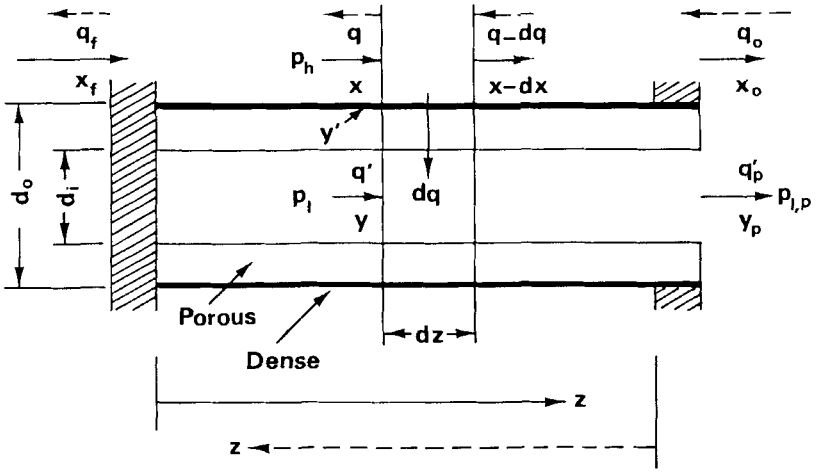

FIG. 1. Schematic of asymmetric hollow fiber membrane separator with cocurrent and countercurrent flows.

TABLE 1
Equations of Material Balances and Permeations

Material Balance

Cocurrent flow		Countercurrent flow	
$Q_f = Q + Q'$	(1a)	$Q = Q_o + Q'$	(1b)
$x_f Q_f = xQ + yQ'$	(2a)	$xQ = x_o Q_o + yQ'$	(2b)
$-dQ = dQ'$	(3a)	$-dQ = -dQ'$	(3b)
$-d(xQ) = d(yQ')$	(4a)	$-d(xQ) = -d(yQ')$	(4b)

Permeation Rate

$$-d(xQ) = dS_d(x - Pry') \tag{5}$$
$$-d\{(1-x)Q\} = dS_d\{(1-x) - Pr(1-y')\}/\alpha_0 \tag{6}$$

where

$$S_d = \frac{P_A p_h}{g_f l} S, \qquad S = n\pi d_o z \tag{6-1}$$

dimensionless forms. The permeate fluxes of binary components over the differential membrane area are given as Eqs. (5) and (6) in Table 1. Rearrangement of these equations yields

$$-\frac{dQ}{dS_d} = x - Pry' + \{(1-x) - Pr(1-y')\}/\alpha_0 \tag{7}$$

$$-\frac{dx}{dS_d} = \left(x - Pry' + x\frac{dQ}{dS_d}\right)\Big/ Q \tag{8}$$

Pressure drop in the low-pressure stream is given by

$$-\frac{dPr}{dS_d} = \frac{l}{P_A}\frac{128RTq_f^2 n}{n^2\pi^2 d_o d_i^4 p_h^3}\frac{Q'}{Pr} \tag{9}$$

where $Q' = 1 - Q$ for cocurrent flow and $Q' = Q_o - Q$ for countercurrent flow.

Equations (7), (8), and (9) are the main working equations for predicting the performance of cocurrent and countercurrent flow separators. However, y', which depends on the flow pattern and Models A and B, is necessary to solve these equations. In the case of Model A, integrating Eqs. (3a) and (4a) or Eqs. (3b) and (4b) gives

$$y' = y = \frac{x_i Q_i - xQ}{Q_i - Q} \tag{10}$$

where $x_i = x_f$ and $Q_i = 1$ for cocurrent flow, and $x_i = x_o$ and $Q_i = 1 - \theta$ for countercurrent flow. In the case of Model B, the following equation can be derived using $d(Qx)/dQ = y'$:

$$\frac{y'}{1 - y'} = \alpha_0 \frac{x - Pry'}{1 - x - Pr(1 - y')} \tag{11}$$

Of course, the bulk composition of low-pressure stream y is given by Eq. (10). Equation (11) also expresses the relation of x and y at the point where $q_p' = 0$, i.e., closed ends, in the Model A.

To predict the separation performance, Eqs. (7), (8), and (9) were solved as a boundary-value problem. The initial and boundary conditions for the cocurrent flow mode are

$$x = x_f, \quad y = y_f, \quad Pr = Pr_f, \quad Q = 1 \quad \text{at } S_d = 0 \text{ (closed end)} \tag{12}$$

$$x = x_o, \quad y = y_p, \quad Pr = p_{l,p}/p_h, \quad Q = 1 - \theta \quad \text{at } S_d = S_{dm} \text{ (open end)} \tag{13}$$

where $y = y_f$ is obtained from Eq. (11) and $Pr = Pr_f$ is an assumed value. Calculations from the closed end to the open end were repeated until Pr became equal to $p_{l,p}/p_h$. For the countercurrent flow mode, similar calculations were carried out from the closed end to the open end with the following initial and boundary conditions:

$$x = x_o, \quad y = y_o, \quad Pr = Pr_o, \quad Q = 1 - \theta \quad \text{at } S_d = S_{dm} \text{ (closed end)} \tag{14}$$

$$x = x_f, \quad y = y_p, \quad Pr = p_{l,p}/p_h, \quad Q = 1 \quad \text{at } S_d = 0 \text{ (open end)} \tag{15}$$

where all initial conditions have unknown values prior to calculation. The gas viscosity, which is dependent on the gas composition, was estimated by Wilke's equation (*21*).

Experimental

The asymmetric hollow fiber membrane of a polyimide supplied by UBE Industries was used for separation tests of H_2-CO mixtures. The fiber has a ultrathin dense layer on the outside, and its outside and inside diameter are around 390 and 220 μm (Table 2). The membrane bundle was made of 6 fibers of 143 cm active length with the open ends of the fibers embedded in a 4.5-cm long metal tube. The bundle was housed in a stainless pipe which had a 2.1 mm i.d. and was 200 cm long in order to reduce the void space around the fibers and obtain the plug flow situation. The gas mixture was fed into the shell side at constant pressure and temperature, and the permeate was withdrawn from the open ends of the fibers at atmospheric pressure. Gas compositions and flow rates were measured by gas chromatography and a soap-film flowmeter.

Results and Discussions

Parametric studies of computer simulation with high selective membranes gave the following results.

(1) Performances differences due to model variations do not appear in the range of small stage cuts, but clearly exist over the range of moderate stage cuts.
(2) Marked differences appear in the reject stream composition rather than in the permeate stream composition.
(3) The factors which produce large pressure drops in the fiber bore, i.e., small i.d. and large length of fiber, large x_f and small ratio of $p_{l,p}/p_h$, decrease the differences of the performances.

Considering Result (*3*) and the accuracy of measurements, we set the experimental conditions.

TABLE 2
Dimensions of Miniature and Pilot Modules

	Miniature	Pilot
Number of fibers	6	8,700
Average d_i (μm)	212	220
Average d_o (μm)	389	390
Active length (cm)	143	150
Membrane area (cm^2)	105	160,000

Figures 2 and 3 shows the results of separations of H_2-CO mixture at p_h = 0.592, $p_{l,p}$ = 0.101 MPa, and T = 373 K with cocurrent and countercurrent flows. The lines in these figures are calculated values of the models using permeabilities determined by matching the measured data of the experiment at the smallest stage cut. This matching method is needed because the pure gas permeability ratio (H_2/CO = 63 in this case) did not reflect the permeations of the mixture. This phenomenon has been often observed in glassy polymer membranes (*22*, *23*). As can be seen from Figs. 2 and 3, there are marked differences between the experimental results measured with cocurrent and countercurrent flow modes above a stage cut of 0.35, and the countercurrent flow mode is superior. Fairly good agreement is obtained between the experimental and the calculated values by Model A but not of Model B. This is clearly

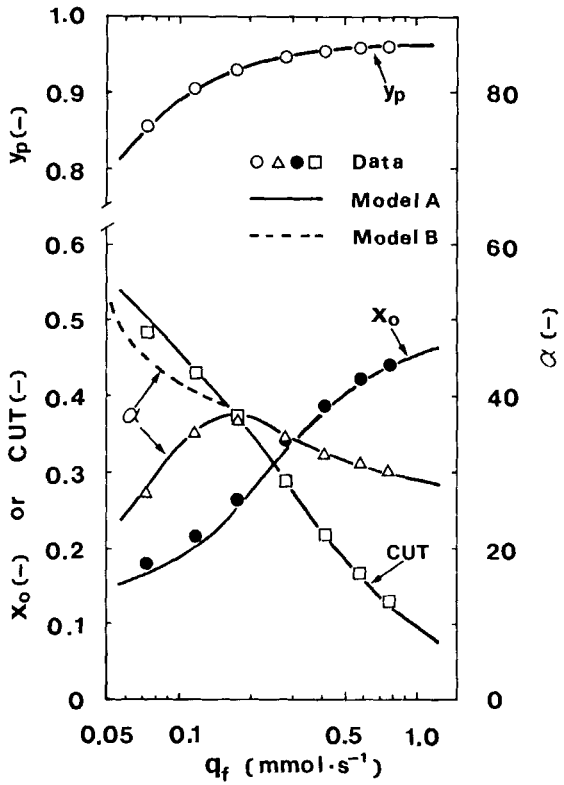

FIG. 2. Effect of feed flow rate on performance of miniature separator with cocurrent flow mode. System parameters: α_0 = 52, P_A/l = 67 nmol·s^{-1}·m^{-2}·Pa^{-1}, p_h = 0.592 MPa, $p_{l,p}$ = 0.101 MPa, T = 373 K, and x_f = 0.505.

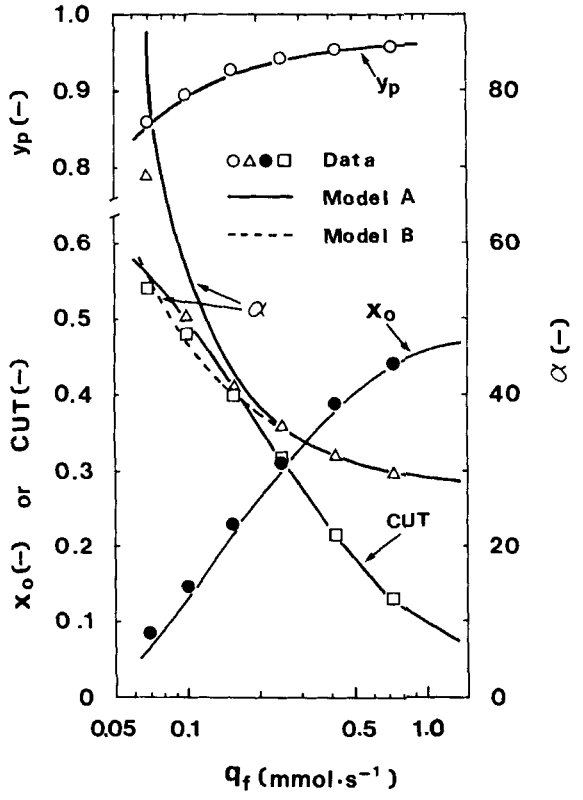

FIG. 3. Effect of feed flow rate on performance of miniature separator with countercurrent flow mode. System parameters: $\alpha_0 = 52$, $P_A/l = 67$ nmol · s^{-1} · m^{-2} · Pa^{-1}, $p_h = 0.592$ MPa, $p_{l,p} = 0.101$ MPa, $T = 373$ K, and $x_f = 0.505$.

represented by the stage separation factor α in the results of the cocurrent flow mode. The validity of Model A is emphasized by the following discussion.

The largest permeate flux measured in this experiment was approximately 0.02 cm/s. For applying Model A, it is an indispensable condition that the mass transfer coefficient in the porous sublayer is greater than in the permeate flux. There is no information available regarding the mass transfer coefficient, but we can roughly estimate it by using the gas diffusivities reported with microporous membranes. The Knudsen diffusion coefficient of nitrogen through Millipore VM whose pore size is 50 nm lies around 0.06 cm^2/s (*24*), and that of a microporous polysulfone membrane lies around 0.002 cm^2/s (*25*). The mass transfer coefficients in

the 100 μm thick microporous membranes are estimated as approximately 6 and 0.2 cm/s, respectively, which are one or two orders of magnitude greater than the permeate flux measured in this experiment.

The results obtained indicate that the mathematical model using the conventional assumptions regarding y and constant permeability can be used for analysis of the separator with a high-flux asymmetric polyimide membrane, while adjustment of the permeabilities is needed at one point of the stage cut. Although Assumption (5) is not theoretically reasonable for glassy polymer membranes, the permeabilities determined by the matching method give good approximations as long as concentration variations are not too large.

ANALYSIS OF A PILOT SCALE SEPARATOR

Experimental and Results

To examine the suitability of the asymmetric polyimide membrane for the separation of hydrogen, a pilot plant was operated using synthetic gases supplied by a coal gasification process. The synthetic gas was fed after removal treatment of acid gases, and its composition was approximately 46% H_2, 53% CO, and 1% N_2. The membrane fibers bundle of 6 cm o.d. was made of 8700 fibers of 150 cm active length, and it was housed in a shell of 8.9 cm i.d. The separator was operated in the countercurrent flow mode with various feed rates, pressure ratios, and temperatures to obtain information on the stability of performance.

The membrane module maintained the initial properties during a test run of over three months. Two examples of the results are shown in Figs. 4 and 5, which indicate that 44% recovery of hydrogen with a purity of 97% at T = 323 K and 62% recovery of hydrogen with a purity of 91% at T = 373 K are attained in these experiments. It was found that the pilot separator has excellent performance and the module mode of the asymmetric polyimide membrane is suitable for separations of hydrogen from various industrial gases.

Analysis by a Serial Multistage Model

In the following, the performance of the pilot separator is analyzed by a modeling study. As can be seen from Figs. 4 and 5, stage separation factors, which were defined by the ratio of H_2/CO fraction of the

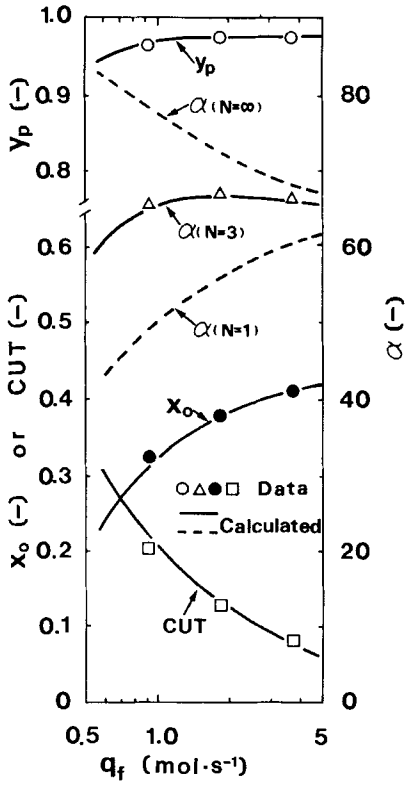

FIG. 4. Performance of pilot separator at T = 323 K. Other system parameters: α_0 = 113, P_A/l = 24.4 nmol · s^{-1} · m^{-2} · Pa^{-1}, p_h = 3.04 MPa, $p_{l,p}$ = 0.592 MPa, and x_f = 0.456.

permeate to that of the reject stream, are approximately equal regardless of the stage cut variations. This is markedly different from the results obtained with the miniature separator, and suggests the existence of longitudinal mixing in the shell side stream of the pilot separator. We attempted to analyze the degree of the mixing by using the serial multistage model illustrated in Fig. 6.

In a separator divided into N spaces with equivalent volumes, the shell side stream (high pressure) is assumed to have complete mixing and the low-pressure stream through the fiber bore is assumed to have plug flow. Since the synthetic gas used can be considered to be a H_2-CO binary mixture, the material balance around the first to the Nth section is

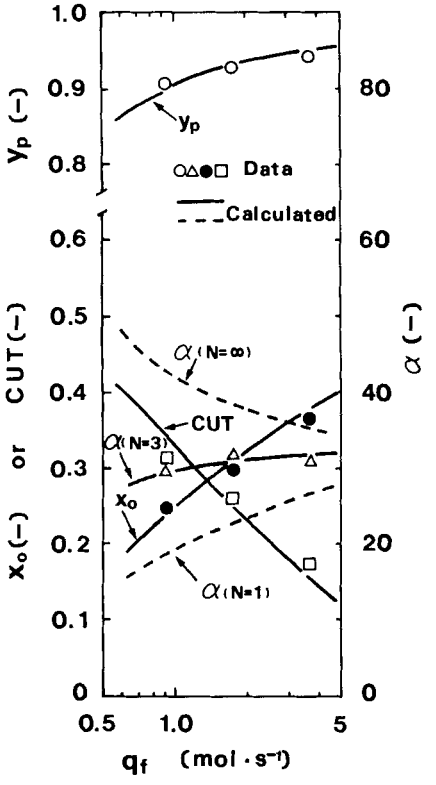

FIG. 5. Performance of pilot separator at T = 373 K. Other system parameters: α_0 = 62, P_A/l = 60.3 nmol · s^{-1} · m^{-2} · Pa^{-1}, p_h = 3.04 MPa, $p_{l,p}$ = 0.69 MPa, and x_f = 0.465.

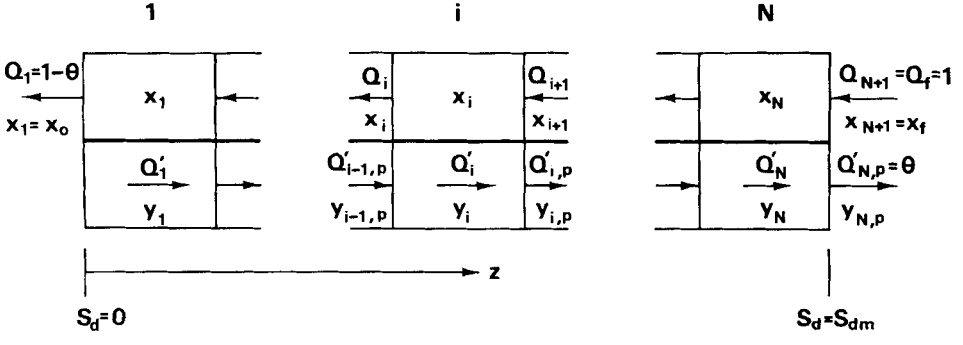

FIG. 6. Schematic of serial multistage model.

$$\theta y_{N,p} = x_f - x_o(1 - \theta) \tag{16}$$

and that around the first to the ith section is

$$Q'_{i,p}y_{i,p} = x_{i+1}Q_{i+1} - x_o(1 - \theta) \tag{17}$$

Differential permeate fluxes in the ith section are given by forms similar to Eqs. (5) and (6). Rearranging those equations yields

$$\frac{dQ'_i}{dS_d} = x_i - Pry_i + \{1 - x_i - Pr(1 - y_i)\}/\alpha_0 \tag{18}$$

$$\frac{dy_i}{dS_d} = \left(x_i - Pry_i - y_i \frac{dQ'_i}{dS_d}\right) \Big/ Q'_i$$

$$dy_i/dS_d = 0 \qquad (Q'_i \neq 0) \tag{19}$$

where x_i is the constant composition of the high-pressure stream in the ith section and y_i is a variable composition of the permeate leaving the interface between the dense layer and the porous layer. The value of y_i was taken as the bulk low-pressure stream taking account of the results of the miniature separator. The pressure drop in the fiber bore is written in the same form as Eq. (9). Equations (18), (19), and (9) were solved as a boundary-value problem as follows.

At first, N and the total stage cut, θ, were assumed, and then the integration was carried out from $S_d = 0$ in the first section with the initial conditions of assumed x_1 and Pr to the point $S_d = S_{dm}/N$. The calculation of the next section was performed after the value of x_i was replaced with the one determined by Eq. (17). Until the values of x_{N+1}, $Q_{N,p}$, and Pr obtained at $S_d = S_{dm}$ became equal to x_f, θ, and $p_{l,p}/p_h$, calculations were repeated from the first to the Nth section.

Calculated results which exhibit good agreement with the experimental results were obtained when N was 3, and they are shown in Figs. 4 and 5 by solid lines. The system parameters used are indicated in the figure legends. The results of the limiting cases, that is, ideal plug flow is assumed ($N = \infty$) or complete mixing is assumed ($N = 1$) over the whole length, are shown by the dashed lines. The performance of the pilot separator is superior to that of the one side mixing model ($N = 1$) but is inferior to that of the case where $N = \infty$. It is expected that the performance will increase considerably by minimizing the longitudinal mixing in the shell side stream of the separator. Investigations on the

ideal plug flow situation by improvements of the arrangement of membranes, locations of the gas inlet and outlet, reduction of the void space, etc. are continuing.

CONCLUSION

The separation performances of high-flux asymmetric polyimide membranes were studied experimentally and theoretically.

1) Experimental results of a miniature module made up of hollow fibers exhibited superiority in the countercurrent flow mode compared to the cocurrent flow mode. These results were in good agreement with the calculated results from a mathematical model which had been used for predicting the performances of symmetric membranes.

2) A pilot plant test demonstrated the suitability of the polyimide membrane for hydrogen separation processes. However, analysis of its performance required taking into account the longitudinal mixing in the shell side stream.

SYMBOLS

d_i	inside diameter of hollow fiber (m)
d_o	outside diameter of hollow fiber (m)
l	effective thickness of selective dense layer (m)
N	number of sections divided into equivalent volume
n	number of hollow fibers
P	gas permeability ($\text{mol} \cdot \text{m} \cdot \text{s}^{-1} \cdot \text{m}^{-2} \cdot \text{Pa}^{-1}$)
Pr	pressure ratio, p_l/p_h
p_h	pressure of high side (Pa)
p_l	pressure of low side (Pa)
Q	dimensionless flow rate of high-pressure stream, q/q_f
Q'	dimensionless flow rate of low-pressure stream, q'/q_f
q	flow rate of high-pressure stream (mol/s)
q'	flow rate of low-pressure stream (mol/s)
R	gas constant ($\text{J} \cdot \text{K}^{-1} \cdot \text{mol}^{-1}$)
S	membrane area (m^2)
S_d	dimensionless membrane area defined by Eq. (6-1)
S_{dm}	total dimensionless membrane area
T	temperature (K)
x	mole fraction of Component A on high-pressure stream
y	mole fraction of Component A on low-pressure stream

y' mole fraction of Component A leaving dense layer
z length of hollow fiber and axial coordinate (m)

Greek

α stage separation factor, $y_p(1 - x_o)/\{(1 - y_p)x_o\}$
α_0 permeability ratio, P_A/P_B
θ stage cut, q_p/q_f
η gas viscosity (Pa · s)

Subscripts

A more permeable component
B less permeable component
f inlet of high-pressure stream
i ith section
N Nth section
o outlet of high-pressure stream
p outlet of permeate stream

Acknowledgments

The authors are deeply indebted to UBE Industries for providing the membranes, and they gratefully acknowledge the contribution of UBE Ammonia Co. in the operation of the pilot plant.

This work is a part of the results of the "C_1 Chemistry Project," a National Research and Development Program of the Agency of Industrial Science and Technology, Ministry of International Trade and Industry (M.I.T.I.), Japan.

REFERENCES

1. S. Weller and W. A. Steiner, *Chem. Eng. Prog., 46,* 585 (1950).
2. R. W. Nayler and P. O. Backer, *AIChE J., 1,* 95 (1955).
3. J. Oishi, Y. Matsumura, K. Higashi, and C. Ike, *J. At. Energy Soc. Jpn., 3,* 923 (1961).
4. S. A. Stern and W. P. Walawender, *Sep. Sci., 4,* 129 (1969).
5. W. P. Walawender and S. A. Stern, *Ibid., 7,* 553 (1972).
6. C. T. Blaisdell and K. Kammermeyer, *AIChE J., 18,* 1015 (1972).
7. C. T. Blaisdell and K. Kammermeyer, *Chem. Eng. Sci., 28,* 1249 (1973).
8. C. Y. Pan and H. W. Habgood, *Ind. Eng. Chem., Fundam., 13,* 323 (1974).

9. S. T. Hwang and K. Kammermeyer, *Membranes in Separations*, Wiley-Interscience, New York, 1975.
10. J. M. Thorman, H. Rhim, and S. T. Hwang, *Chem. Eng. Sci., 30,* 751 (1975).
11. C. R. Antonson, R. J. Gardner, C. F. King, and D. Y. Ko, *Ind. Eng. Chem., Process Des. Dev., 16,* 463 (1977).
12. S. A. Stern and S. C. Wang, *J. Membr. Sci., 4,* 141 (1978).
13. C. Y. Pan and H. W. Habgood, *Can. J. Chem. Eng., 56,* 510 (1978).
14. A. Sengupta and K. K. Sirker, *J. Membr. Sci., 21,* 73 (1984).
15. J. E. Perrin and S. A. Stern, *AIChE J., 31,* 1167 (1985).
16. Y. Shindo, T. Hakuta, H. Yoshitome, and H. Inoue, *Sep. Sci. Technol., 20,* 445 (1985).
17. R. T. Chern, W. J. Koros, and P. S. Fedkiw, *Ind. Eng. Chem., Process Des. Dev., 24,* 1015 (1985).
18. C. Y. Pan, *AIChE J., 29,* 545 (1983).
19. A. S. Berman, *J. Appl. Phys., 24,* 1232 (1953).
20. K. Haraya, T. Hakuta, H. Yoshitome, and S. Kimura, *Sep. Sci. Technol., 22,* 1425 (1987).
21. C. R. Wilke, *J. Chem. Phys., 18,* 517 (1950).
22. R. T. Chern, W. J. Koros, E. S. Sanders, and R. Yui, *J. Membr. Sci., 15,* 157 (1983).
23. R. T. Chern, W. J. Koros, B. Yui, H. B. Hopfenberg, and V. T. Stannett, *J. Polym. Sci., Polym. Phys. Ed., 22,* 1061 (1984).
24. H. Yasuda and J. T. Tsai, *J. Appl. Polym. Sci., 18,* 805 (1974).
25. I. Cabasso, K. Q. Robert, E. Klein, and J. K. Smith, *Ibid., 21,* 1883 (1977).

Received by editor March 16, 1987